GEOPHYSICAL RESEARCH LETTERS, VOL. 35, L21601, doi:10.1029/2008GL035753, 2008

South Equatorial Undercurrent in the western to central tropical Atlantic

Jürgen Fischer,[1] Verena Hormann,[1] Peter Brandt,[1] Friedrich A. Schott,[1] Benjamin Rabe,[2] and Andreas Funk[1]

Received 20 August 2008; revised 24 September 2008; accepted 1 October 2008; published 7 November 2008.

[1] The South Equatorial Undercurrent (SEUC) in the western to central tropical Atlantic is investigated by a combination of shallow floats, with a few acoustically tracked, shipboard current measurements and hydrography. Float trajectories show a well confined SEUC revealing large standing meanders near its western origin. Transports determined from 31 sections across the SEUC increase from 5.6 Sv at 35°W near the western boundary to 10.2 Sv 800 km farther east. Internal recirculations north and south of the SEUC were indicated by the float trajectories and a weak transport reduction farther along its eastward progression is observed. The deep part of the South Equatorial Current carries on both sides of the SEUC interior water masses westward, and supplies almost 5 Sv to the SEUC between 35°W and 28°W, or about half of the SEUC transport in the interior tropical Atlantic.
Citation: Fischer, J., V. Hormann, P. Brandt, F. A. Schott, B. Rabe, and A. Funk (2008), South Equatorial Undercurrent in the western to central tropical Atlantic, *Geophys. Res. Lett.*, *35*, L21601, doi:10.1029/2008GL035753.

1. Introduction

[2] The shallow circulation of the tropical Atlantic consists of a complex system of zonal current bands fed by the meridional circulation along the western boundary. The most prominent of these is the Equatorial Undercurrent that is supplied by water masses of South Atlantic origin through the retroflection of the North Brazil Current. On either side of the equator, there are additional subsurface current bands transporting water away from the western boundary toward the eastern upwelling regions. Herein we are interested in the southern band, the South Equatorial Undercurrent (SEUC), and we will concentrate on investigations regarding its origin, transports, and supply routes.

[3] Already in 1979 *Cochrane et al.* [1979, p. 724] stated: "In each hemisphere of the Atlantic, a permanent countercurrent having a core about 4.5° from the equator is present in the subthermocline layer. Although currents along the Brazilian coast supply water to the countercurrents, much of the flow in each seems to be internal to the anticyclonic region on its equatorward side". Previous investigations of the shallow tropical circulation [*Schott et al.*, 1998, 2003] showed SEUC transports across 35°W and on the basis of oxygen distributions it was argued that some of the supply is of southern origin as is supported by *Goes et al.* [2005]. On the larger scale the observations along the transatlantic section at 4° 30'S [*Arhan et al.*, 1998; *Marin and Gouriou*, 2000; *Bourlès et al.*, 2002] provide insights into the regional structure of the SEUC. The most prominent feature of the pycnocline is its eastward rise to the surface which occurs approximately at the Greenwich Meridian and the poleward deflection of the South and North Equatorial Undercurrents. The largest thickness of the zonal flow was observed near 20°W [*Marin and Gouriou*, 2000, Figure 5] and there is an apparent cessation of the SEUC near 5°W.

[4] In its Pacific counterpart, called Southern Subsurface Countercurrent (SSCC), *Rowe et al.* [2000] found a sharp and strong reversal of relative vorticity over a distance of 20 km at the core of the SSCC and a sharpened potential vorticity (PV) front. This front separates a region of very low homogeneous PV on the equatorward side from a homogeneous high PV region on the poleward side. *Rowe et al.* [2000, p. 1172] further state: "Each potential vorticity pool extends well beyond the edges of the SSCC into regions of westward flow".

[5] Numerical models of the tropical Atlantic Ocean have been used for investigating the structure and physical mechanisms of the off-equatorial undercurrents: *Jochum and Malanotte-Rizzoli* [2004] suggested by using an idealized model configuration that eddy fluxes induced by tropical instability waves maintain the SEUC in the central equatorial Atlantic. In a more realistic high-resolution simulation of the Atlantic Ocean, *Hüttl-Kabus and Böning* [2008] noted that the SEUC in the western part of the equatorial Atlantic is almost exclusively fed by internal recirculations between eastward and westward current bands.

2. SEUC Flow From Float Trajectories

[6] Within the framework of the German Clivar Program (2000–2004; 9 floats) and later through the German Argo contribution (2004–2006; 12 floats) profiling APEX floats were deployed in the western tropical Atlantic to support the investigations of the shallow tropical circulation. These floats were ballasted to drift at 200 m depth. In regular 10 day intervals these floats descend down to 1500 m (2000 m for the 2004 deployments) depth from which they subsequently rise to the surface and collect temperature and salinity profiles measured by a Seabird CTD. After a period of 11 to 15 hours at the surface they sink down to their 200 m park level to begin a new cycle. Two of the profiling floats in the area were equipped with an acoustic receiver

[1] IFM-GEOMAR, Leibniz-Institut für Meereswissenschaften, Kiel, Germany.
[2] Alfred-Wegener-Institut für Polar- und Meeresforschung, Bremerhaven, Germany.

0094-8276/08/2008GL035753$05.00

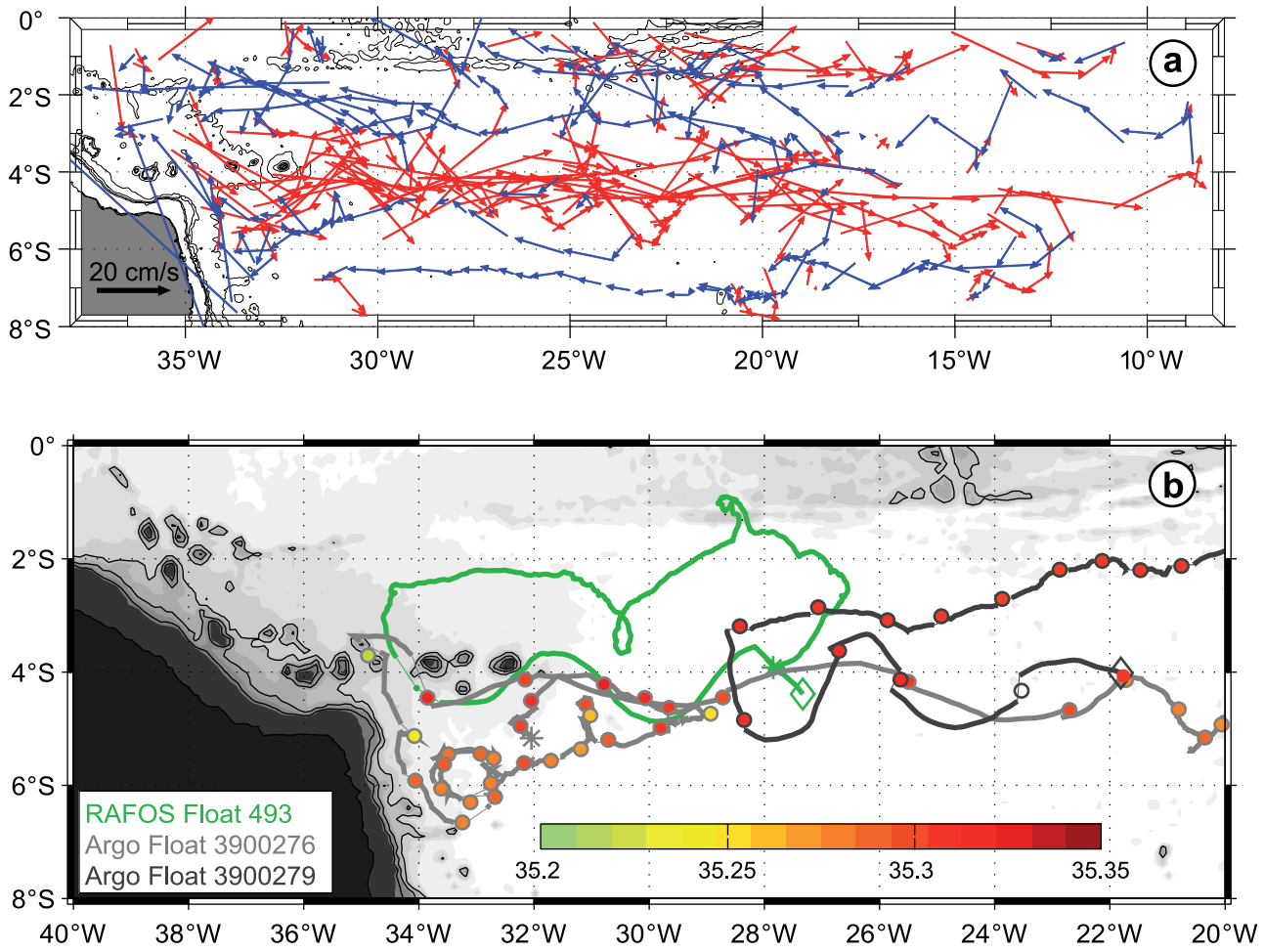

Figure 1. (a) Current velocities from 10 profiling Argo floats drifting at 200 m depth; launch times in year 2000 and 2004; the Atol das Rocas is shown near 4°S, west of 32°W. Eastward flow is in red and westward is in blue. Bottom topography is included. (b) Trajectories of acoustically tracked floats drifting at the 200 m level (deployed at the locations marked by asterisks and last position given by diamond), and salinities on $\sigma_\theta = 26.6$ kgm^{-3} are shown as colored circles (see colorbar) at surfacing locations of the profiling Argo floats.

for detecting RAFOS sound signals and thus could be tracked, while underwater. Several floats deployed south of the equator and near the boundary entered a narrow band of eastward flow (Figure 1a), the SEUC. In its westernmost part the flow is not strictly zonal, but large meridional excursions appear, with the northern limit of the meanders just south of the seamount chain (Atol das Rocas). North and south of the SEUC the flow is westward suggesting a relatively deep penetration of the different branches of the South Equatorial Current (SEC). In addition, the surface drift, detected during the data transmission periods is also westward above the SEUC.

[7] Altogether from the float data we obtained 174 estimates (10 day averages) of the zonal flow in the latitude band 3°S to 6°S and from the shelf break at 35°W out to approximately 10°W, a distance of more than 2500 km. The mean zonal (eastward) velocities calculated for this band are 16.5 cms^{-1} west of 28°W, 17.9 cms^{-1} for the area 28°W to 23°W, and 13.4 cms^{-1} east of 23°W; calculated by only taking eastward flow into account for the mean SEUC speed. More details are available from the two acoustically tracked APEX floats and one non-profiling RAFOS float. These allow determining float velocities at park levels twice a day, which in the core of the SEUC occasionally reach 50 cms^{-1}. Apparently, the floats turn to westward direction at various locations, e.g., near 28°W, 20°W, 17°W and the last float leaves the SEUC near 10°W either via a northern or southern route, and the reason for this is not clear yet. Some rationale for such a behavior is seen in the zonal flow along 4.5°S measured during the French CITHER1 cruise in 1993 [*Arhan et al.*, 1998]. Along that section some evidence of the meandering in the western part is apparent and there is increasing strength of the flow out to approximately 15°W and weakening farther into the basin. At about 10°W to 6°W the flow appears much weaker and the velocity maximum is much closer to the surface with only weak flow at the 200 m level. This eastward rise is much more pronounced in their oxygen distribution, where the SEUC core is marked by an intermediate O_2-maximum. The small number of floats available, and the possibility of an artifact caused by the isobaric float behavior, prevents to make firm statements about the fate of the SEUC in the central and eastern Atlantic. However, there are indications that interior recirculation loops of the SEUC/SEC flow exist

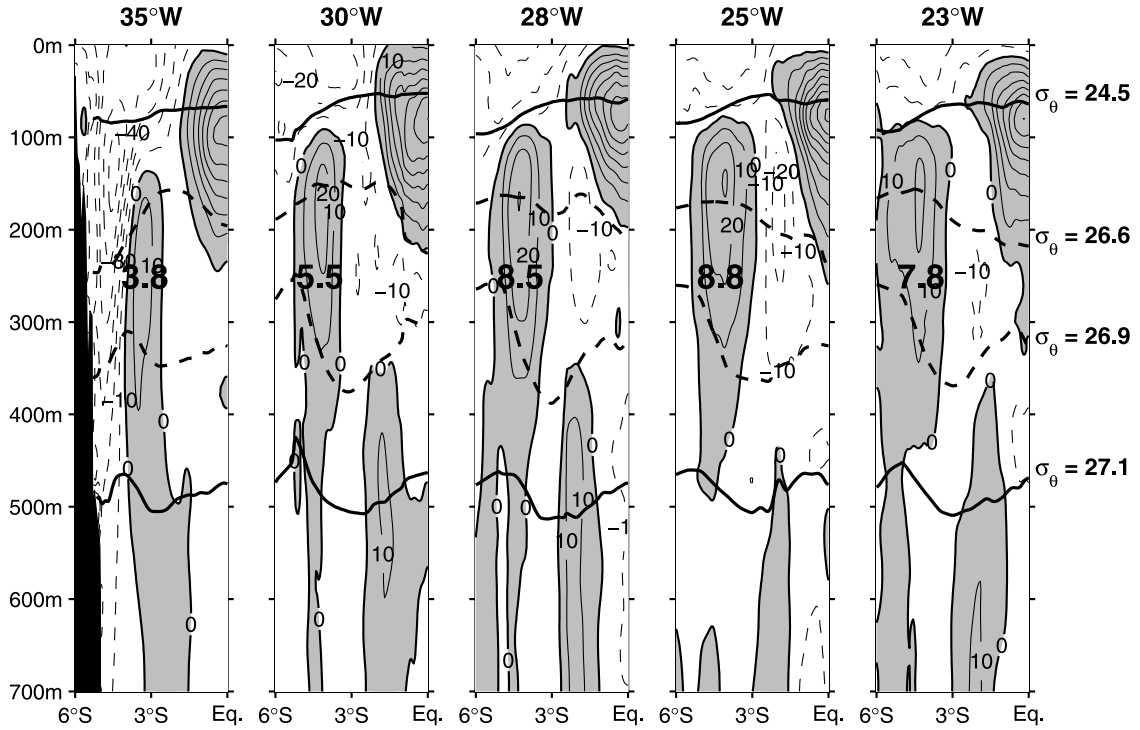

Figure 2. Mean sections of zonal flow at 35°W (14 occupations), 30°W (4 occupations), 28°W (5 occupations), 25°W (4 occupations), and 23°W (4 occupations) from a combination of shipboard and lowered ADCP data. The time span is from 1990 to 2008; isotach interval is 10 cms^{-1}; bold numbers are transports in Sverdrup ($1Sv = 10^6 m^3 s^{-1}$); isopycnals are included as thick solid (σ_Θ = 24.5 and 27.1 kgm^{-3}) and dashed (σ_Θ = 26.6 and 26.9 kgm^{-3}) black lines, respectively.

at both sides along the path of the SEUC from its origin toward the center of the basin.

3. SEUC Water Masses and Their Origin

[8] Three float trajectories are displayed in Figure 1b to show the principle water mass paths, with two profiling ones tracked by RAFOS sound sources and a third non-profiling RAFOS float (green curve in Figure 1b). The latter was deployed in late August 2004 at 4°S and its surfacing was observed very close to the deployment position in mid-April 2005. This RAFOS float left the SEUC shortly after deployment and followed the SEC to the western boundary where it was entrained again into the SEUC, performing a meandering eastward excursion. Another path is illustrated by the southern profiling float (float 3900276 in Figure 1b). This float was deployed in August 2004 south of the SEUC near 5°S, 32°W. It first followed the SEUC which was left to the south near 29°W and afterwards it slowly drifted westward. Near the western boundary it was then entrained into the North Brazil Undercurrent (NBUC) flowing north until it re-entered the SEUC near 35°W and north of Atol das Rocas. This float shows the lowest salinities (quality controlled data) and exhibits considerable salinity variability along its path. One has to keep in mind that these floats are isobaric drifters, and the isopycnic depth variations of the relevant isopycnic surfaces near the western boundary are not negligible. South of the islands this float roughly followed the same meander structure revealed by the RAFOS float. The third float (float 3900279, March to July 2006 visible in Figure 1b) came from the east and shows a swift westward progression north of the SEUC, presumably following the deep part of the SEC or the southern extension of the Equatorial Intermediate Current [see, e.g., *Schott et al.*, 2003]. This float exhibits the highest salinities with only weak variations. It enters the SEUC in the interior of the tropical Atlantic near 29°W, indicating that the SEUC is at least partially supplied by interior pathways. Salinities from CTD station data of the corresponding cruises in March 2000, May 2002 and August 2004 (not shown here) also support this. The total range of salinities on σ_θ = 26.6 kgm^{-3} was quite narrow, from 35.0 to 35.4 with the lowest salinities, below 35.2, found along the coastal flank of the NBUC and strong gradients occurred across the NBUC. At the offshore flank of the NBUC at 5° 30'S salinities above 35.25 were observed and these are also present in the SEUC band near 3°S, 35°W.

4. SEUC Transports From Ship Sections

[9] Meridional sections with shipboard and lowered ADCPs were carried out since the WOCE period along 35°W (14 cruises), near 30°W (4 cruises), 28°W (5 cruises), near 25°W (4 cruises), and 23°W (4 cruises); see Table 1, as well as, for example, *Schott et al.* [1998, 2003], *Brandt et al.* [2006], and *Hormann and Brandt* [2007]. Most of the sections covered the total vertical extent of the SEUC at different times of the year; but only at 35°W all seasons are covered. The mean flow across each of the sections (Figure 2) was calculated by averaging the gridded individual realizations as an Eulerian mean flow field. At 35°W the SEUC is only weakly developed at a mean core speed of

Table 1. SEUC Transport in Sv[a] in the Western to Central Tropical Atlantic, for the Potential Density Range σ_θ = 24.5–27.1 kgm^{-3}, and in the Depth Range 100 m to 500 m

Cruise	σ_θ	Depth
35°W		
L'Atalante-(Feb.93)	8.0	8.0
Ron Brown-(Feb. 02)	5.6	5.4
Meteor 27/3-(Mar. 94)	3.7	3.6
Meteor 47/1-(Apr. 00)	8.7	9.3
E.A. Link-(Apr. 96)	8.9	9.5
Meteor 53/2-(May 02)	3.7	4.3
Sonne 171-(May 03)	5.0	4.7
Meteor 16/3-(Jun. 91) [100–400m]	(2.9)[c]	3.7[b] (1.28)
Meteor 68/2-(Jun. 06)	4.0	4.1
Thalassa-(Jul. 99)	4.3	4.3
Meteor 62/2-(Aug. 04)	6.6	6.5
Meteor 14/2-(Oct. 90)	6.1	6.3
Meteor 22/2-(Nov. 92)	3.7	3.9
Sonne 152-(Dec. 00)	4.6	4.6
Mean for n = 13 (σ_θ), n = 14 (depth)	5.6	5.7
Uncertainty of mean	0.5	0.5
30°W–31°W		
M. Ewing-(Mar. 94) [100–400m]	(5.1)[c]	5.4[b] (1.03)
James Clark Ross-(May 07)		6.9
Meteor 16/3-(Jun. 91)	5.4	5.5
Meteor 62/2-(Aug. 04)		8.5
Mean for depth range (n = 4)		6.7
Uncertainty of mean		0.7
28°W		
S. Johnson-(Jan. 00)	9.5	9.4
Meteor 53/2-(May 02)	9.9	10.1
Sonne 170-(May 03)	10.3	10.4
Polarstern-(May 08) [100–250m]		4.6[b] (1.61)
Meteor 62/2-(Aug. 04)	11.2	11.0
Mean for n = 4 (σ_θ), n = 5 (depth)	10.2	9.7
Uncertainty of mean	0.4	0.6
25°W–26°W		
S. Johnson-(Jan. 00)	4.8	4.8
Ron Brown-(Feb. 05)	10.2	10.0
Meteor 34/4-(Mar. 96) [100–450m]	(11.2)[c]	12.9[b] (1.01)
Ron Brown-(Aug. 03)	10.4	10.4
Mean for n = 3 (σ_θ), n = 4 (depth)	8.4	9.6
Uncertainty of mean	1.8	1.7
23°W		
S. Johnson-(Jan. 00)	8.6	8.7
Meteor 47/1-(Apr. 00)	10.7	10.6
Polarstern-(Jun. 05) [100–300m]		6.0[b] (1.23)
Thalassa-(Aug. 99)	5.1	5.0
Mean for n = 3 (σ_θ), n = 4 (depth)	8.1	7.9
Uncertainty of mean	1.6	1.2

[a]A sverdrup is 10^6 m^{3}s^{-1}.
[b]Reduced depth range; scaled by factor in brackets for calculating the mean.
[c]For density range σ_θ = 24.5–26.9 kgm^{-3}; not used in mean.

about 10 cms^{-1} and the onshore flank is bounded by the intense north-westward flowing NBUC; thus the SEUC is shifted more to the north, compared to the SEUC location at the other sections, and centered around 3°S. Besides the zonal component, there are several realizations [see *Schott et al.*, 1998] showing a significant southward (opposite to the NBUC direction) component. Toward the east, already at 30°W and more pronounced at 28°W, the SEUC is significantly stronger (maximum mean speed is above 20 cms^{-1}), and its width and vertical extent are larger than near the boundary at 35°W. This is also reflected in the intensification of the zonal flow determined from the float displacements (Figure 1). East of 35°W the SEUC core is located slightly south of 4°S. Additionally, the flow at 23°W appeared weaker, but wider than farther west, with slightly less mean SEUC transports compared to 28°W (Table 1). The mean transports were derived by averaging the individual section transport estimates, and uncertainties were calculated from the transport standard deviations and the number of (independent) section occupations. In order to incorporate the few data sets with somewhat shallower measurement range, a scaling factor was determined to take that into account. At the respective locations, full range measurements were used to determine full SEUC transports, and secondly, transports over the reduced depth range were derived. The ratio of the two estimates was then used to upscale the transports from the shallower data sets. Quantitatively, the SEUC transports increase significantly (see error estimates in Table 1) from 5.6 Sv near the western boundary at 35°W to about 10 Sv 800 km farther east. We have chosen two types of vertical boundaries for the transport calculations, isopycnals ($24.5 < \sigma_\theta \leq 27.1$ kgm^{-3}; see Figure 2 and Table 1) and depth range (100–500 m); both give roughly the same values. In order to uniformly capture the full SEUC transports from the western boundary to the interior, we have chosen an isopycnal range, which is somewhat wider than that used by *Schott et al.* [1998] for the western boundary only.

[10] East of 28°W, the transports of the SEUC remain almost constant, with some insignificant reduction in the area 25°W to 23°W. Although the reduction is weak and supported by only a few realizations at each of these sections, it is in agreement with the velocity decrease determined solely from the floats.

[11] In contrast to this method we also calculated transport averages as was done by *Brandt et al.* [2006] from the mean (Eulerian) velocity sections of Figure 2, which should be somewhat smaller than the average core transports listed in Table 1. Particularly, the 35°W transports from the mean velocity section are 3.8 Sv compared to 5.6 Sv and thus by about 30% smaller, which is an indication of relatively large variability in the position of the current core at this location. Large variability and large differences between the two methods point to meandering as the primary source of the variability at 35°W. At 28°W, the scatter of core location is much smaller, and the transport estimates are more similar, at 8.5 Sv and 10.2 Sv, respectively (Table 1). Presumably, meandering is less dominant and SEUC pulsation may add to the variability. Finally, at 23°W transports scatter quite significantly, but means are rather similar (7.8 Sv vs. 8.1 Sv) again making pulsations more likely than meandering.

5. SEUC Meandering Near the Western Boundary

[12] A very interesting and to our knowledge so far unknown SEUC feature is the apparently standing wave in its westernmost part. This is shown by the float-based current vectors and the RAFOS trajectories in Figures 1a and 1b, where different floats from different years and seasons seem to follow almost the same wavelike pattern. The western meander trough envelopes the island of Fer-

nando de Noronha, and the subsequent ridge of the SEUC meander is located north of the latitude of the island. Unfortunately, our 5°S sections are located too far south to fully resolve these meanders and the meridional sections have a too large spacing to resolve this structure. However, with the float vectors as guidance we see some meander-evidence in the shipboard current measurements.

[13] Further support of the meander pattern can be derived from climatological hydrography [*Gouretski and Koltermann*, 2004], revealing a series of high and low PV pools (not shown) in the area of the SEUC origin.

6. Summary and Conclusions

[14] The SEUC in its western part shows a series of meanders that are present in both, individual float trajectories (Figures 1a and 1b) and in the distribution of climatological mean PV. Near its origin at 35°W the SEUC transport is fairly well determined to be 5.6 ± 0.5 Sv and it increases substantially during its eastward progression; at 28°W the transport has almost doubled, and then stays fairly constant (just a slight decay) out to 23°W. This transport variation is caused by a significant increase in SEUC volume and core velocity. Floats clearly show the interior recirculation north of the SEUC, including a very nice example of a closed trajectory loop east of 35°W. In addition, there are also floats that retroflect to the south, drifting westward with the southern SEC and either re-enter the SEUC farther west or feed the NBUC. In terms of water mass signals we see a clear distinction of interior saline water and much fresher water carried north by the NBUC [*Schott et al.*, 1998] (Figure 1b), while the offshore flank of the NBUC carries rather saline water of interior origin.

[15] How do present-day models of high resolution represent the SEUC? Both types of models, idealized as by, for example, *Jochum and Malanotte-Rizzoli* [2004], and high-resolution models with realistic forcing as by, for example, *Hormann and Brandt* [2007] and *Hüttl-Kabus and Böning* [2008], show eastward SEUC flow at the observed latitude, but current speeds and transports are weaker than observed. In the model run presented by *Hüttl-Kabus and Böning* [2008] the SEUC at its western origin is mainly fed from the north by the westward SEC flow, turning southward near 35°W. Stable (i.e., significant in the annual mean) meanders evolve east of 35°W and there is a seasonal variation in the SEUC strength with maximum flow in boreal summer.

[16] Both, *Hüttl-Kabus and Böning* [2008] and *Jochum and Malanotte-Rizzoli* [2004] found that the upper SEUC flow appears not to be connected to the western boundary, but supplied through interior recirculations. This is what our observations also suggest by comparing the almost nonexistent SEUC above σ_θ = 26.6 kgm^{-3} at 35°W (Figure 2) with the strong eastward flow in the same layer, but farther east. On the other hand, oxygen maxima have been reported in the SEUC farther east [*Schott et al.*, 1998; *Tsuchiya*, 1986], and recent observations at 23°W [*Brandt et al.*, 2008] show an oxygen maximum in the deeper part (around 400 m depth) of the SEUC indicating either a direct connection to the western boundary flow or recirculation of oxygen-rich water from the south. It is this deeper part of the equatorial circulation that is not well represented in these models, but which might play an important role for the supply of oxygen-rich waters to the eastern oxygen minimum zones.

[17] **Acknowledgments.** The study was supported by the German Science Foundation through Scho 168/30, FI 871/1-1, and various *Meteor* cruises, and by the German Bundesministerium für Bildung und Forschung (BMBF, German Argo-Tropat, and RV *Sonne* cruises). We would further like to thank PIs of the various US, French, and German cruises.

References

Arhan, M., H. Mercier, B. Bourlès, and Y. Gouriou (1998), Hydrographic sections across the Atlantic at 7°30 N and 4°30 S, *Deep Sea Res., Part I*, *45*, 829–872.

Bourlès, B., M. D'Orgeville, G. Eldin, R. Chuchla, Y. Gouriou, Y. du Penhoat, and S. Arnault (2002), On the evolution of thermocline and subthermocline eastward currents in the eastern equatorial Atlantic, *Geophys. Res. Lett.*, *29*(16), 1785, doi:10.1029/2002GL015098.

Brandt, P., F. A. Schott, C. Provost, A. Kartavtseff, V. Hormann, B. Bourlès, and J. Fischer (2006), Circulation in the central equatorial Atlantic: Mean and intraseasonal to seasonal variability, *Geophys. Res. Lett.*, *33*, L07609, doi:10.1029/2005GL025498.

Brandt, P., V. Hormann, B. Bourlès, J. Fischer, F. A. Schott, L. Stramma, and M. Dengler (2008), Oxygen tongues and zonal currents in the equatorial Atlantic, *J. Geophys. Res.*, *113*, C04012, doi:10.1029/2007JC004435.

Cochrane, J. D., F. J. Kelly Jr., and C. R. Olling (1979), Subthermocline counter-currents in the western equatorial Atlantic Ocean, *J. Phys. Oceanogr.*, *9*, 724–738.

Goes, M., R. L. Molinari, I. da Silveira, and I. Wainer (2005), Retroflections of the North Brazil Current during February 2002, *Deep Sea Res., Part I*, *52*, 647–667.

Gouretski, V. V., and K. P. Koltermann (2004), *WOCE Global Hydrographic Climatology* [CD-ROM], *Rep. 35*, 52 pp., Bundesamt für Seeschifffahrt und Hydrogr., Hamburg, Germany.

Hormann, V., and P. Brandt (2007), Atlantic Equatorial Undercurrent and associated cold tongue variability, *J. Geophys. Res.*, *112*, C06017, doi:10.1029/2006JC003931.

Hüttl-Kabus, S., and C. W. Böning (2008), Pathways and variability of the off-equatorial undercurrents in the Atlantic Ocean, *J. Geophys. Res.*, *113*, C10018, doi:10.1029/2007JC004700.

Jochum, M., and P. Malanotte-Rizzoli (2004), A new theory for the generation of the equatorial subsurface countercurrents, *J. Phys. Oceanogr.*, *34*, 755–771.

Marin, F., and Y. Gouriou (2000), Heat fluxes across 7°30′N and 4°30′S in the Atlantic Ocean, *Deep Sea Res., Part I*, *47*, 2111–2139.

Rowe, G. D., E. Firing, and G. C. Johnson (2000), Pacific equatorial subsurface countercurrent velocity, transport, and potential vorticity, *J. Phys. Oceanogr.*, *30*, 1172–1187.

Schott, F. A., J. Fischer, and L. Stramma (1998), Transports and pathways of the upper-layer circulation in the western tropical Atlantic, *J. Phys. Oceanogr.*, *28*, 1904–1928.

Schott, F. A., M. Dengler, P. Brandt, K. Affler, J. Fischer, B. Bourlès, Y. Gouriou, R. L. Molinari, and M. Rhein (2003), The zonal currents and transports at 35°W in the tropical Atlantic, *Geophys. Res. Lett.*, *30*(7), 1349, doi:10.1029/2002GL016849.

Tsuchiya, M. (1986), Thermostads and circulation in the upper layer of the Atlantic, *Prog. Oceanogr.*, *16*, 235–267.

P. Brandt, J. Fischer, A. Funk, V. Hormann, and F. A. Schott, IFM-GEOMAR, Leibniz-Institut für Meereswissenschaften, Düsternbrooker Weg 20, D-24105 Kiel, Germany. (jfischer@ifm-geomar.de)

B. Rabe, Alfred-Wegener-Institut für Polar- und Meeresforschung, Bussestrasse 24, D-27570 Bremerhaven, Germany.